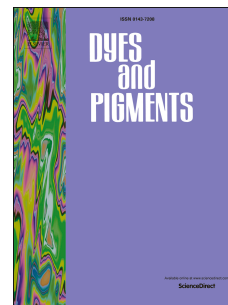


# Journal Pre-proof

Water-soluble near-infrared fluorescent probes enhanced by ionic co-assembly of a four-armed amphiphile with SDBS: Toward application in cell imaging

Lina Zhang, Shixin Zhou, Shenxi Min, Xiaobo Yu, Guangliang Hou, Qin Tong, Bin Dong, Huifang Zhu, Bo Song



PII: S0143-7208(19)33001-3

DOI: <https://doi.org/10.1016/j.dyepig.2020.108541>

Reference: DYPI 108541

To appear in: *Dyes and Pigments*

Received Date: 22 December 2019

Revised Date: 2 May 2020

Accepted Date: 10 May 2020

Please cite this article as: Zhang L, Zhou S, Min S, Yu X, Hou G, Tong Q, Dong B, Zhu H, Song B, Water-soluble near-infrared fluorescent probes enhanced by ionic co-assembly of a four-armed amphiphile with SDBS: Toward application in cell imaging, *Dyes and Pigments* (2020), doi: <https://doi.org/10.1016/j.dyepig.2020.108541>.

This is a PDF file of an article that has undergone enhancements after acceptance, such as the addition of a cover page and metadata, and formatting for readability, but it is not yet the definitive version of record. This version will undergo additional copyediting, typesetting and review before it is published in its final form, but we are providing this version to give early visibility of the article. Please note that, during the production process, errors may be discovered which could affect the content, and all legal disclaimers that apply to the journal pertain.

© 2020 Published by Elsevier Ltd.

**Lina Zhang:** Writing - original draft, Data curation, Investigation. **Shixin Zhou:** Formal analysis. **Shenxi Min:** Formal analysis. **Xiaobo Yu:** Resources. **Guangliang Hou:** Formal analysis. **Qin Tong:** Data curation. **Bin Dong:** Resources. **Huifang Zhu:** Resources. **Bo Song:** Conceptualization, Supervision, Project administration, Writing - review & editing.

Journal Pre-proof

**Water-soluble near-infrared fluorescent probes enhanced by ionic co-assembly of a four-armed amphiphile with SDBS: toward application in cell imaging**

Lina Zhang,<sup>a</sup> Shixin Zhou,<sup>b</sup> Shenxi Min,<sup>a</sup> Xiaobo Yu,<sup>a</sup> Guangliang Hou,<sup>a</sup> Qin Tong,<sup>a</sup> Bin Dong,<sup>c</sup> Huifang Zhu\*<sup>d</sup>, Bo Song\*<sup>a</sup>

---

<sup>a</sup> *College of Chemistry, Chemical Engineering and Materials Science, Soochow University, Suzhou 215123, P. R. China. E-mail: songbo@suda.edu.cn*

<sup>b</sup> *Department of Cell Biology and Stem Cell Research Center, School of Basic Medical Sciences, Peking University Health Science Center, Beijing 100191, P. R. China*

<sup>c</sup> *Jiangsu Key Laboratory for Carbon-Based Functional Materials & Devices, Soochow University, Suzhou, 215123, P. R. China.*

<sup>d</sup> *Analysis and Testing Center, Soochow University, Suzhou, 215123, P. R. China. E-mail: hfzhu@suda.edu.cn*

**Keywords**

Near-infrared fluorescence

Ionic co-assembly

Emission enhancement

Aggregation-induced emission

Cell imaging

## Abstract

Near-infrared (NIR) organic fluorescent probes have attracted great deal of attention for application in cell imaging, where the probes demand good water solubility, strong emission and good cytocompatibility. In this study, a conjugate of anthraquinone and tetraphenylethylene is introduced into an amphiphile (denoted by BTPEAQ-10) with four pyridinium terminated aliphatic chains. The assemblies of BTPEAQ-10 show an NIR emission peaked at 670 nm. Ionic co-assembly with sodium dodecyl benzene sulfonate leads to drastic enhancement of the fluorescent emission to 30-fold. Controlling experiments on different surfactants and anionic groups show that both the hydrophilic group and the alkyl chain play critical role to the emission enhancement. Both the assemblies and co-assemblies have good water solubility and cytocompatibility, and were applied in cell imaging. The co-assemblies showed much better contrast of cell imaging due to the higher emission property.

## 1. Introduction

Supramolecular assembly presents a versatile platform for tuning the emission of fluorescent dyes, and thus owns great potential in preparation of fluorescent probes applicable in the field of cell imaging.[1-4] Among them, fluorophores with near-infrared (NIR) emission are developing rapidly owing to their advantages, such as overcoming the auto-fluorescence of the bio-systems,[5-7] reducing photo-damage,[8, 9] and providing deeper tissue penetration[10, 11] relative to fluorophores in the short-wavelength region.[12-17] Cells contain a large quantity of water as well as organelles and lipid membranes. Thus, the organic fluorescent dyes, as being applied as probes in the cells, inevitably aggregate due to their inherent hydrophobic nature.[18, 19] Therefore, good water-solubility and strong emissive property are requisite

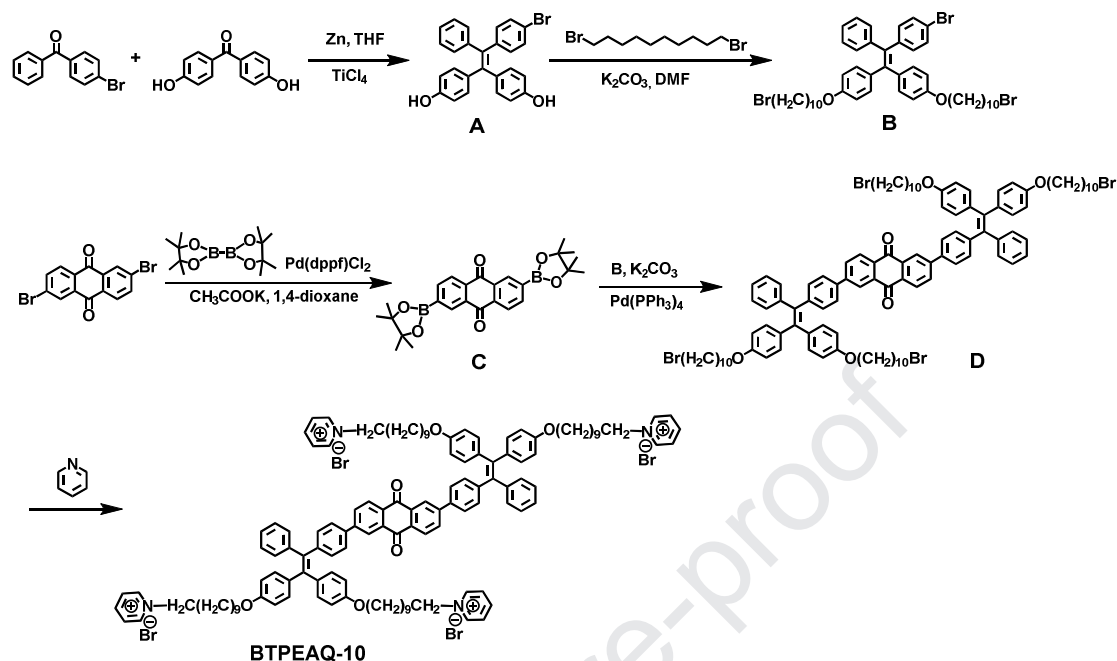
in their aggregated state for labelling the cells.[20, 21] On this regard, marriage of supramolecular assembly and fluorescent dyes with aggregation-induced emission (AIE) properties would produce new fluorescent probes that meet the requirement of applications in cell imaging.[22-24]

To obtain NIR emission, narrow band gap dyes are classically realized by extending  $\pi$ -conjugation system,[25, 26] or introducing strong donor-acceptor groups to the aromatics.[27, 28] For the traditional fluorescent dyes, a big  $\pi$ -system often suffers from the aggregation-caused quenching of fluorescence emission.[29-32] On this regard, the AIE dyes show great advantages, and such kinds of dyes usually own big Stokes shift, which are favoured for application as probes in biosystems.[33-35] Recently, Bin Liu et al. reported a NIR AIE dots, which is composed of fluorescent dyes by conjugating one anthraquinone and two tetraphenylethylene (TPE) groups. This molecule shows rather weak fluorescent emission. However, encapsulation by DSPE-PEG block copolymer or silica colloids led to strong emission and efficient singlet oxygen.[28]

Ionic co-assembly has been demonstrated an effective method to tune the emission in terms of intensity and wavelength,[36-42] which was usually realized by changing the packing mode or the distance of  $\pi$ -plane.[43-47] For instance, Arun K. Nandi et al. found that the controllable co-assembly of ionic surfactants with opposite charges could be used to turn on/off reversible fluorescence of ionic agglomerates.[48] Subodh Kumar et al. showed the possibility of enhancing the emission intensity by ionic assembly far below the critical micelle concentration (CMC) of the surfactants.[49]

In this study, we introduced the AIE dyes designed by Bin Liu et al.[28] as a core to an amphiphile with four pyridinium terminated alkyl chains, and attempted to tune the emission by ionic co-assembly through adding a second amphiphile. It turns out that both the assemblies and co-assemblies have good water solubility, and the latter showed 30-fold higher intensity of NIR emission compared to the former. Controlling experiments on different amphiphiles and salts show that both the hydrophilic group and the alkyl chain play critical role

to the emission enhancement. The co-assemblies have excellent cytocompatibility and were successfully applied on HeLa cells imaging.



**Scheme 1.** The synthetic route of BTPEAQ-10.

## 2. Results and discussion

The synthetic route of BTPEAQ-10 is illustrated in Scheme 1. The details of synthesis are shown in the experimental section, and the corresponding  $^1\text{H}$  NMR and mass spectra (MS) are shown in electronic supplementary information (ESI). BTPEAQ-10 has good solubility in methanol, and moderate solubility in water. Being dissolved in methanol, BTPEAQ-10 showed an emission peak at around 425 nm, excited by 340 nm light. Keeping the concentration of BTPEAQ-10 ( $C_B$ ) at  $1 \times 10^{-5} \text{ mol L}^{-1}$ , and adding water into the solution resulted in the decrease of the emission intensity. At the same time, a new peak appeared at around 670 nm, which covered from 520 to 840 nm. The intensity of the new peak increases with the water fraction ( $f_w$ , by volume) in methanol. The new emission peak should be attributed to the aggregation of BTPEAQ-10. The enhanced emission accords well with the AIE property of BTPEAQ,[28] reported by Liu et al. The peak intensity at 670 nm is plotted against  $f_w$ , as shown in Fig. 1. The emission did not show observable increase

until  $f_w$  was approximately 60%, and thereafter increased drastically, and then increased slowly as  $f_w$  was more than 90%. It is worth to note that the aggregation of BTPEAQ-10 led to the Stokes shift of 240 nm, and the whole emission peak is far away from the excitation light (340 nm). The absorption band has a little overlap with the emission band (Fig. S1). Therefore, the auto-absorption is negligible. These features make the aggregated BTPEAQ-10 suitable for application in cell imaging or other bio-related labelling.

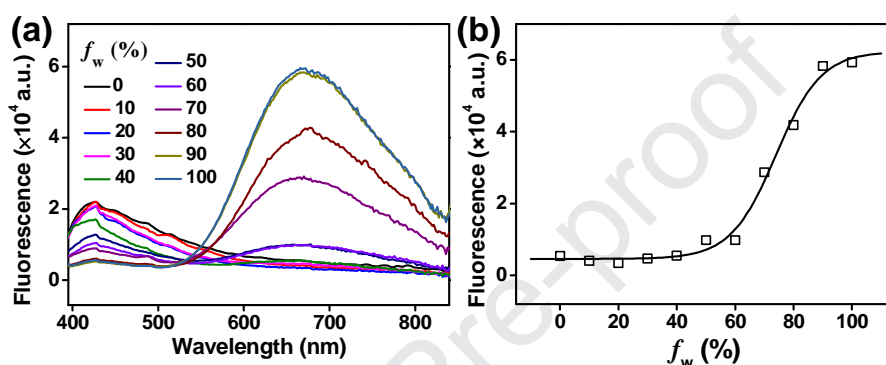


**Fig. 1.** (a) Fluorescence spectra of BTPEAQ-10 with different  $f_w$ . (b) Plot of fluorescence intensity at 670 nm versus  $f_w$ .  $C_B = 1 \times 10^{-5}$  mol L $^{-1}$ ,  $\lambda_{ex} = 340$  nm.

Utilizing the AIE property, we are able to determine the CMC of BTPEAQ-10. The fluorescent intensity was plotted versus the corresponding concentration, as shown in Fig. 2. Linear fitting of the data showed an intersection at around  $6.6 \times 10^{-7}$  mol L $^{-1}$ , which should correspond to the CMC. This result is understandable. Below the CMC, BTPEAQ-10 does not form micelles (small bundles of molecules may happen), and hence the fluorescence at 670 nm is very weak and increases slowly with concentration; above the CMC, the fluorescence increases drastically due to the formation of micelles.

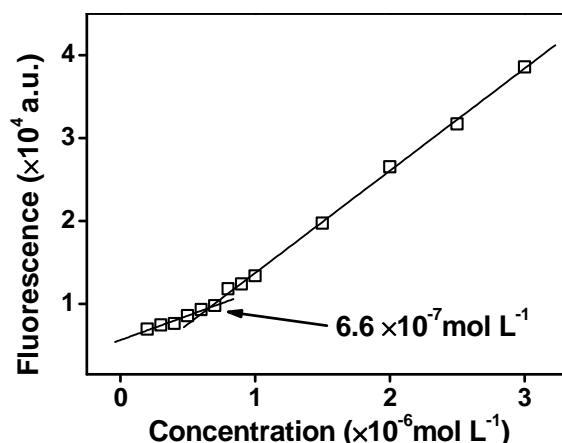


**Fig. 2.** Plot of fluorescence intensity versus the corresponding concentration.  $\lambda_{\text{ex}} = 340 \text{ nm}$ .

During the study, we found an interesting phenomenon. The fluorescence was significantly enhanced upon addition of sodium dodecyl benzene sulfonate (SDBS), as shown in Fig. 3a (where the molar concentration of SDBS ( $C_S$ ) was 4-fold of  $C_B$ ). The emission difference can also be observed by the pictures of the solutions excited by 365 nm UV light (inset of Fig. 3a). As shown in Fig. 3b, plotting of the peak intensity versus the molar ratio of  $C_S / C_B$  (denoted by  $R$ ) shows an intersection at 4. As  $R \leq 4$ , the emission intensity increases drastically with  $R$ ; as  $R > 4$ , the increase slows down. We assume that the interaction between each cationic alkyl chain on BTPEAQ-10 and anionic SDBS has no association effect, and hence the combination of BTPEAQ-10 with one SDBS molecule will not make another combination of SDBS molecule easier or more difficult. As  $R > 4$ , most of the BTPEAQ-10 molecules are involved in the complexation, and pushing the equilibrium to right side needs more SDBS molecules. The fluorescence enhancement was also evaluated by photoluminescence quantum yield (PLQY). The PLQY of neat BTPEAQ-10 solution (above CMC) is 0.3% and increases to 2.9% as adding 4-fold SDBS (i.e.  $R = 4$ ). The fluorescence enhancement also brings about the changes of average lifetimes ( $\tau_{\text{aveS}}$ ). The  $\tau_{\text{aveS}}$  are 1.12 and 4.16 ns for neat BTPEAQ-10 and co-assemblies of BTPEAQ-10 & SDBS, respectively. The corresponding transient fluorescence spectra are shown in Fig. S3. With these values, we are able to estimate

the radiative and non-radiative decay rates (the calculation is presented in the ESI). The radiative decay rates increased from  $2.68 \times 10^{-3}$  to  $6.98 \times 10^{-3}$ , and the non-radiative decay rates reduced from 0.89 to 0.23 (Table. S1) upon addition of SDBS into BTPEAQ-10 aqueous solution.

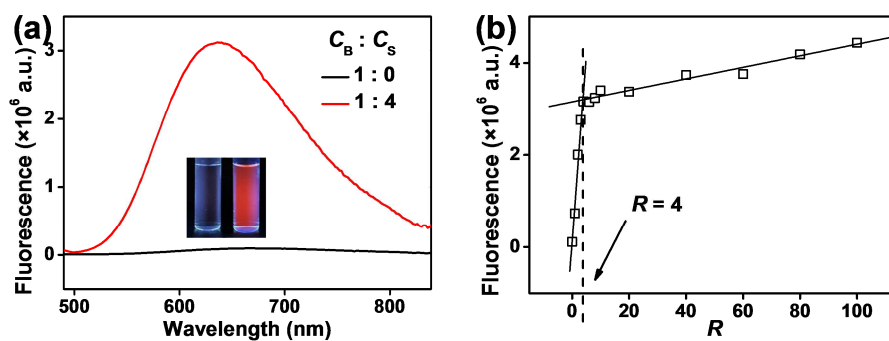


**Fig. 3.** (a) Fluorescence spectra of BTPEAQ-10 in absence and presence of 4-fold SDBS in aqueous solution. Inset: Photographs of the corresponding solution under illumination of 365 nm light. (b) Plot of fluorescence intensity at 670 nm versus  $C_S$ .  $C_B = 1 \times 10^{-5} \text{ mol L}^{-1}$ ,  $\lambda_{\text{ex}} = 340 \text{ nm}$ .

The complexation between BTPEAQ-10 and SDBS was investigated by MS. As shown in Fig. 4, the mass-to-charge ratios show peaks at 710.42, 1228.51 and 2783.48, corresponding to the complexes of BTPEAQ-10@SDBS, BTPEAQ-10@(SDBS)<sub>2</sub> and BTPEAQ-10@(SDBS)<sub>3</sub>. The experimental isotopic peaks are consistent with the theoretical simulation. It is worth to note that these three groups of peaks are all found for the solutions with different  $R$ . We did not find the peaks of complexes of BTPEAQ-10@(SDBS)<sub>4</sub>, but we assume that this complex should also exist in the solution. The absence from the spectra is because that the charge of the co-assembly is neutralized when binding 4 molecules of SDBS on BTPEAQ-10. These results confirm that the complexation between BTPEAQ-10 and SDBS has no association effect. Based on the above results, we conclude that the addition of SDBS into the aqueous solution of BTPEAQ-10 will produce 4 kinds of complexes, as shown in Fig. 4d. The increase of the amount of SDBS will push the equilibrium to right side, and thus the complexes with more SDBS are formed.

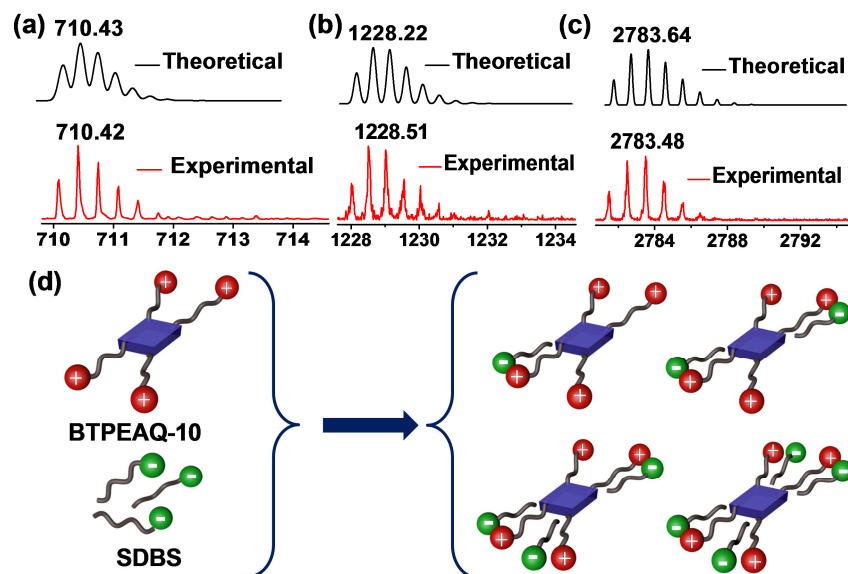


**Fig. 4.** Theoretical simulation and experimental MS of BTPEAQ-10 and SDBS mixture: (a) BTPEAQ-10@SDBS, (b) BTPEAQ-10@(SDBS)<sub>2</sub>, (c) BTPEAQ-10@(SDBS)<sub>3</sub>, (d) Schematic illustration of the possible complexes formed by BTPEAQ-10 and SDBS.

The ionic interaction between BTPEAQ-10 and SDBS was verified by Fourier transform infrared (FTIR) spectra. As shown in Fig. 5, the two characteristic peaks of sulfonate group at around 1133 and 1045  $\text{cm}^{-1}$  are assigned to the antisymmetric and symmetric stretching vibration, respectively. Upon complexation, the peak at around 1133  $\text{cm}^{-1}$  shifted to 1130  $\text{cm}^{-1}$ , and the single peak at 1045  $\text{cm}^{-1}$  split to double peaks at 1045 and 1036  $\text{cm}^{-1}$ . The spectral changes should be attributed to the electrostatic interaction between sulfonate and pyridinium groups.

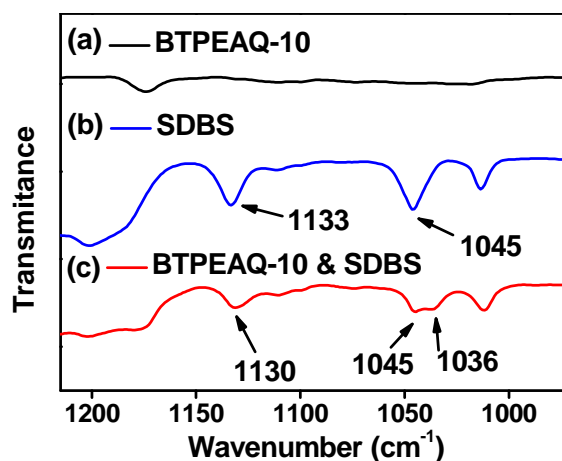


**Fig. 5.** FTIR spectra of (a) BTPEAQ-10, (b) SDBS and (c) mixture of BTPEAQ-10 &

SDBS ( $R = 4$ ).

We were wondering whether the complexation has effect on the assembly of BTPEAQ-10, and thus we investigated the morphologies of the aggregates of BTPEAQ-10 before and after addition of SDBS. Atomic force microscopy (AFM) images are shown in Fig. 6, and grain-like nanostructures are observed on silicon substrate, which should stand for the micellar aggregates formed by BTPEAQ-10 in the aqueous solution. The apparent sizes of the grains are length of 50 - 100 nm, width of 30 - 60 nm and height of 5 - 25 nm. Upon addition of SDBS, the grain-like structures are converted to spherical structures. Particle analysis shows an average lateral diameter of 170 nm, in range of 40 - 360 nm. The height is in range of 20 - 45 nm. We speculate that the co-assemblies of BTPEAQ-10 and SDBS formed spherical structures in the solution, and these structures collapsed during the drying process. This makes a reasonable explanation to the big difference of the diameter and height. Transmission electron microscope (TEM) showed similar structures, as shown in Fig. S5. The morphological changes can also be reflected by the increased intensity in the whole spectra and stronger scattering of the co-assemblies formed by BTPEAQ-10 and SDBS indicated by UV-vis absorption spectra and Tyndall effect (Fig. S6), respectively. Both the assembly and the co-assembly have good stability, and there is no collapse, cracking or other morphological changes during storage (as shown in Fig. S7).

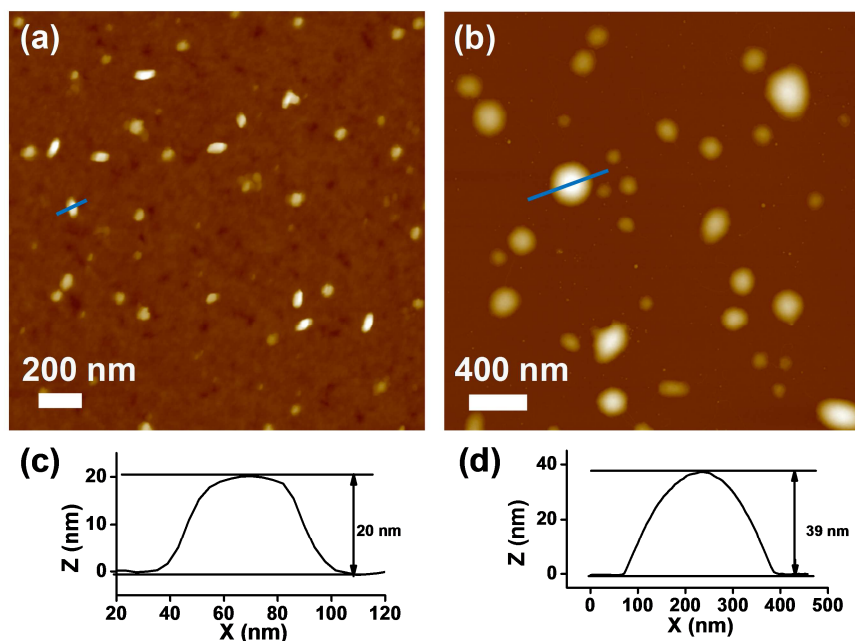


**Fig. 6.** AFM images of (a) the assemblies BTPEAQ-10 and (b) co-assemblies of BTPEAQ-10 and SDBS. Section analysis of (c) the assemblies BTPEAQ-10 and (d) co-assemblies of BTPEAQ-10 and SDBS ( $R = 4$ ).

The photostability of the probes is one of the most important concerns. As shown in Fig. S8, we investigated the photostability of BTPEAQ-10 and co-assemblies of BTPEAQ-10 & SDBS ( $R = 4$ ). The results show that after irradiating with a 365 nm ultraviolet (12 W) for 40 minutes, the emission of BTPEAQ-10 hardly changes, which means that BTPEAQ-10 has excellent photostability. For the co-assemblies of BTPEAQ-10 & SDBS, the emission showed a little decrease after being continuously irradiation. Based on the above two groups of experiment, we conclude that dissociation might happen upon irradiation.

The co-assembly of BTPEAQ-10 and SDBS mainly relies on electrostatic and hydrophobic interaction. Therefore, the formation of the co-assembly can also be reflected by the changes in zeta potential ( $\zeta$ ). The  $\zeta$ s were 44.7 and -29.3 mV for the assemblies of BTPEAQ-10 and co-assemblies of BTPEAQ-10 & SDBS ( $R = 4$ ), respectively. The  $\zeta$  conversion further confirms the complexation and co-assembly of BTPEAQ-10 and SDBS in the aqueous solution.

Except for SDBS, we also testified the effect of other surfactants and anionic groups on the emission of BTPEAQ-10. Herein, sodium dodecyl sulfonate (SDS), sodium laurate (SL), sodium stearate (SS), sodium p-toluene sulfonate (SpTS), sodium mesitylenesulfonate (SMes), sodium 3-nitrobenzene sulfonate (S3-NBS), sodium methanesulfonate (SMS), sodium trifluoromethanesulfonate (STFMS), sodium acetate (NaAc) and sodium bromide (NaBr) were selected for investigation. The corresponding chemical structures are shown in Table S2. The intensity of the fluorescence at 670 nm is plotted versus the categories of anionic groups. As shown in Fig. 7,  $F_0$  and  $F$  are the initial emission and the emission of BTPEAQ-10 after adding different amounts of additives. Addition of SDBS ( $R = 4$ ) resulted in approximately 30-fold enhancement of fluorescent emission, while addition of SDS, SL, SS caused approximately 15-fold, 5.5-fold, 6.0-fold enhancement, respectively. In contrast, the rest anionic groups showed a little effect on the fluorescence of BTPEAQ-10. These results indicate that both the tosyl head and alkyl chain are indispensable for the strong emission of BTPEAQ-10.

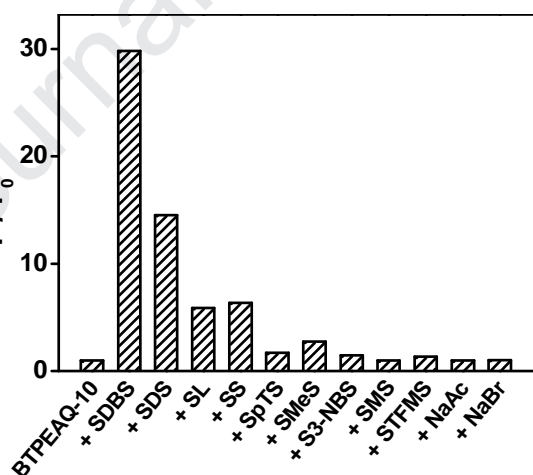


**Fig. 7.** The fluorescence intensity of BTPEAQ-10 at 670 nm versus categories of anionic groups.  $C_B = 1 \times 10^{-5} \text{ mol L}^{-1}$ , and concentration of the additives are  $4 \times 10^{-5} \text{ mol L}^{-1}$ .

Cytocompatibility is a very important parameter for application in labelling the cells. Herein, the cytocompatibility of BTPEAQ-10 and BTPEAQ-10 & SDBS was testified by the cell viabilities. In doing so, cell counting kit-8 (CCK-8) assay was employed to measure the cell viabilities of HeLa cells treated with BTPEAQ-10 and

BTPEAQ-10 & SDBS. Note that the cells were cultured in the mediums with the fluorescent probes for 12 h before being fixed. As shown in Fig.8, the viabilities of HeLa cells were close to 100% as  $C_B < 8 \times 10^{-6} \text{ mol L}^{-1}$ , and start to drop afterward. In case of BTPEAQ-10 & SDBS mixture, the viabilities are much better than the neat BTPEAQ-10, and kept almost 100 % as  $C_B < 12 \times 10^{-6} \text{ mol L}^{-1}$ . These results indicate that both BTPEAQ-10 and BTPEAQ-10 & SDBS have good cytocompatibility.

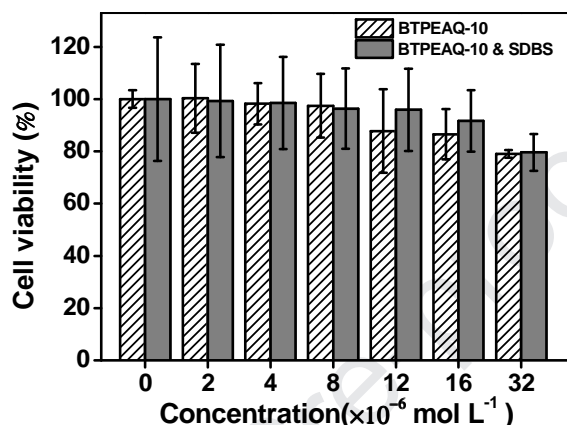


**Fig. 8.** Viability of HeLa cells being cultured in mediums containing BTPEAQ-10 or mixture of BTPEAQ-10 & SDBS.

BTPEAQ-10 and mixture of BTPEAQ-10 & SDBS were applied to label HeLa cells. In the present study, the cells were cultured in the mediums containing the fluorescent probes for 2 h, and then fixed with polyoxymethylene (see the details in the experimental section). Note here, for both probes,  $C_B$  was controlled to be  $5 \times 10^{-6} \text{ mol L}^{-1}$ , far below the toxic dose. As shown by the confocal laser scanning microscope (CLSM) images in Fig. 9, both BTPEAQ-10 and BTPEAQ-10 & SDBS are successfully applied to label the HeLa cells, and showed clear topological structure of the cells, and the latter showed much stronger contrast. These results indicate that the mixture of BTPEAQ-10 & SDBS presents a better NIR probe in cell imaging in comparison of neat BTPEAQ-10.

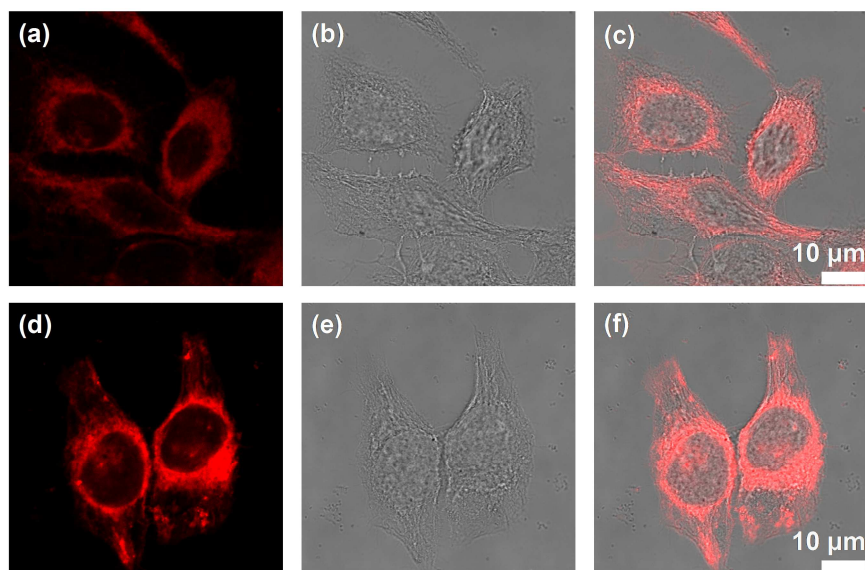


**Fig. 9.** CLSM images of HeLa cells (excitation wavelength: 405 nm): (a-c) cells treated with BTPEAQ-10, (d-f) cells treated with mixture of BTPEAQ-10 & SDBS. From left to right columns are fluorescence, bright field, and merged images.

### 3. Conclusions

In summary, we designed and synthesized an amphiphilic fluorescent probe (i.e. BTPEAQ-10) containing a conjugated group of anthraquinone and TPE. BTPEAQ-10 shows AIE property in aqueous solution and NIR emission covers in range of 520-840 nm. However, the emission is rather weak and the PLQY is merely 0.3%. Co-assembly of BTPEAQ-10 and SDBS can drastically improve the emission, and the PLQY was promoted to 2.9% under existence of 4-fold SDBS. Both the ionic and hydrophobic interactions play important roles in the fluorescent enhancement. The co-assemblies of BTPEAQ-10 and SDBS show better cytocompatibility and high contrast fluorescent images, presenting a good NIR probe in cell imaging.

### 4. Experimental

#### 4.1 Materials

4-Bromobenzophenone,  $\text{CDCl}_3$ ,  $\text{DMSO-}d_6$  were purchased from J&K Chemical Co., Ltd (Shanghai). 4,4'-Dihydroxybenzophenone and 1,10-Dibromodecane were purchased from Energy Chemical Co., Ltd. Zinc powder,  $\text{TiCl}_4$ , Tetrahydrofuran (THF), N, N-dimethylformamide (DMF),

methanol, pyridine, anhydrous  $\text{Na}_2\text{SO}_4$ , anhydrous  $\text{NaCl}$ , anhydrous  $\text{K}_2\text{CO}_3$ ,  $\text{HCl}$ ,  $\text{KAc}$ ,  $\text{NaAc}$ , and  $\text{NaBr}$  were purchased from Sinopharm Chemical Reagent Co., Ltd.  $\text{Pd}(\text{PPh}_3)_4$ , SDBS were purchased from TCI Development Co., Ltd (Shanghai). Ethyl acetate, petroleum ether, dichloromethane (DCM) and chloroform were obtained from Yonghua Chemical Technology Co., Ltd (Jiangsu). 2,6-Dibromoanthracene-9,10-dione was purchased from Bide Pharmaceutical Technology Co., Ltd (Shanghai). 1,4-Dioxane was purchased from 3A Chemicals Co., Ltd.  $\text{Pd}(\text{dppf})\text{Cl}_2 \cdot \text{CH}_2\text{Cl}_2$ , SDS, SL, SS, SpTS, SMeS, S3-NBS, SMS, STFMS were obtained from Macklin Biochemical Technology Co., Ltd. Bis(pinacolato)diboron was obtained from Aladdin Biochemical Technology Co., Ltd (Shanghai). Milli-Q water with resistivity of  $18 \text{ M}\Omega \text{ cm}$  was produced by Direct-Q5uv manufactured by Merck Millipore.

#### 4.2 Instruments

$^1\text{H}$  NMR spectra were recorded on Avance III 400 MHz (Bruker, USA) and 600 MHz NMR spectrometer (Agilent Technologies, USA). MS of the products were obtained on micro Q-TOF III mass spectrometer (Bruker, USA) in the electrospray ionization (ESI) mode and matrix-assisted laser desorption/ionization time-of-flight mass spectroscopy (MALDI-TOF-MS). The MS of complexation between BTPEAQ-10 and SDBS was investigated with the solution of  $R = 20$ . The fluorescence spectra were recorded on FLS980 (Edinburgh Instrument, UK). The UV-vis absorption spectra were recorded on Cary 60 (Agilent Technologies, USA). The PLQYs were obtained by C9920-02G (HAMAMASTU Instrument, Japan) using the integration sphere by absolute method. AFM images were taken on Multimode 8 microscope (Bruker, USA). The peak force quantitative nanomechanical mapping mode with a ScanAasyst-Air probe (nominal spring constants  $0.4 \text{ N m}^{-1}$ , frequency 70 kHz, from Bruker) was adopted during the measurement. The samples were cast on silicon substrates and dried in vacuum. TEM characterization was

performed by FEI TECNAI F20 operating at 200 kV. Approximately 6  $\mu\text{L}$  of sample solution was cast onto a carbon-coated copper grid, and then the grid was dried in vacuum. FTIR spectra were recorded on Nicolet 6700 produced by Thermo Scientific (USA). The cell images were obtained by STP6000 CLSM (LEICA, Germany). Transient fluorescence spectra measurements were carried out by using time-correlated single-photon counting lifetime spectroscopy system (Edinburgh FL920) with a semiconductor laser as the excitation source. The  $\zeta$  measurements were performed at  $25 \pm 0.1$  °C using a Malvern Zetasizer Nano-ZS instrument (Malvern, UK).

#### 4.3 Synthesis and characterization

##### 4.3.1 Synthesis of 4,4'-(2-(4-bromophenyl)-2-phenylethene-1,1-diyl)diphenol (compound A).

Compound A was synthesized following the procedures reported in the literature[50] with some modifications. 4-Bromobenzophenone (3.90 g, 15 mmol), 4,4'-Dihydroxybenzophenone (1.60 g, 7.50 mmol) and zinc powder (4.50 g, 70 mmol) were added to a 250-mL three-necked round-bottom flask. The flask was vacuumed and purged with nitrogen for 3 times. Afterward, 100 mL of anhydrous THF was injected. The reaction system was cooled down to 0 °C, and  $\text{TiCl}_4$  (3.40 mL, 31 mmol) was added dropwise to the mixture. Then the mixture was vigorously stirred in an ice bath for 2 h. Finally, the mixture was refluxed at 78 °C for 24 h. After cooling to room temperature, hydrochloric acid (150 mL, 1 mol  $\text{L}^{-1}$ ) was added. The mixture was stirred for 15 min and then filtered. The filtrate was extracted with DCM for 3 times, and the organic layer was dried with anhydrous sodium sulfate. Then the solvent was removed on a rotavapor. The coarse product was separated by silica gel column chromatography with hexane / ethyl acetate (5:2, v/v) as eluent. The white solid was the final product (1.80 g, yield 54%).  $^1\text{H}$  NMR (400 MHz,  $\text{DMSO}-d_6$ )  $\delta$  9.35 (t,  $J = 15.2$  Hz, 2H), 7.31 (d,  $J = 8.3$  Hz, 2H), 7.12 (dd,  $J = 14.7, 7.3$  Hz,

3H), 6.93 (d,  $J = 7.1$  Hz, 2H), 6.85 (d,  $J = 8.3$  Hz, 2H), 6.73 (t,  $J = 8.3$  Hz, 4H), 6.50 (dd,  $J = 18.5, 8.4$  Hz, 4H).

#### 4.3.2 Synthesis of 4,4'-(2-(4-bromophenyl)-2-phenylethene-1, 1-diyl)bis(((10-bromodecyl)oxy) Benzene (compound B).

Compound B was synthesized following the procedures reported in the literature[51] with some modifications. 1, 10-Dibromodecane (2.40 g, 8 mmol) and  $K_2CO_3$  (1.38 g, 10 mmol) were added to a 100-mL three-necked round-bottom flask. The flask was vacuumed and purged with nitrogen for 3 times. Afterward, 10 mL of anhydrous DMF was injected. The mixture was heated to 70 °C, then the anhydrous DMF (10 mL) containing compound A (0.44 g, 1 mmol) was added dropwise to the mixture. The mixture was refluxed at 70 °C for 20 h. After cooling to room temperature, sodium chloride solution (40 mL) was added. Afterward, the mixture was extracted with DCM, washed with distilled water for 3 times. Then the organic layer was dried with anhydrous sodium sulfate, and the solvent was removed on a rotavapor. The crude product was purified by silica column chromatography with hexane / DCM (5:3, v/v) as eluent. The yellow oily droplet was the final product (0.27 g, yield 31%).  $^1H$  NMR (400 MHz,  $CDCl_3$ )  $\delta$  7.21 (d,  $J = 8.4$  Hz, 2H), 7.09 (t,  $J = 9.3$  Hz, 3H), 7.00 (d,  $J = 7.6$  Hz, 2H), 6.89 (td,  $J = 8.4, 5.9$  Hz, 6H), 6.63 (dd,  $J = 14.1, 8.7$  Hz, 4H), 3.93 - 3.82 (m, 4H), 3.47 (dt,  $J = 49.7, 6.8$  Hz, 4H), 1.90 - 1.69 (m, 8H), 1.43 (s, 8H), 1.30 (s, 16H).

#### 4.3.3 Synthesis of

*2,6-bis(4,4,5,5-tetramethyl-1,3,2-dioxaborolan-2-yl)anthracene-9,10-dione (compound C).*

Compound C was synthesized following the procedures reported in the literature[52] with some modifications. 2,6-dibromoanthracene-9,10-dione (0.76 g, 2.06 mmol), Bis(pinacolato)diboron (1.32 g, 5.20 mmol),  $Pd(dppf)Cl_2 \cdot CH_2Cl_2$  (0.17 g, 0.21 mmol) and KAc (0.73 g, 7.43 mmol) were

added to a 100-mL two-necked round-bottom flask. The flask was vacuumed and purged with nitrogen for 3 times. Then anhydrous 1, 4-dioxane (40 mL) was added to the flask. The mixture was stirred at room temperature for 30 min and refluxed at 84 °C for 40 h. The reactant was cooled down and quenched by adding water (20 mL). Then the mixture was extracted with DCM for 3 times, and the organic phase was dried with anhydrous sodium sulfate. Then the solvent was removed on a rotavapor. The coarse product was separated by silica gel column chromatography with DCM / methyl alcohol (20:1, v/v) as eluent. The primrose powdery was the final product (0.35 g, yield 37%). <sup>1</sup>H NMR (400 MHz, CDCl<sub>3</sub>) δ 8.75 (s, 2H), 8.30 (d, *J* = 7.7 Hz, 2H), 8.20 (d, *J* = 7.7 Hz, 2H), 1.38 (s, 24H).

#### 4.3.4 Synthesis of

*2,6-bis(4-(2,2-bis(4-((10-bromodecyl)oxy)phenyl)-1-phenylvinyl)phenyl)ant-hracene-9,10-dione (compound D).*

Compound B (0.88 g, 1 mmol), compound C (0.18 g, 0.40 mmol) and K<sub>2</sub>CO<sub>3</sub> (0.55 g, 4 mmol) were added to a 250-mL two-necked round-bottom flask. The flask was vacuumed and purged with nitrogen for 3 times, then anhydrous THF (100 mL) and nitrogen-bubbled water (20 mL) were added to the flask. After the mixture was purged with nitrogen for 30 min, Pd(PPh<sub>3</sub>)<sub>4</sub> (46.20 mg, 0.04 mmol) was added. Then the mixture was refluxed at 75 °C for 72 h. After cooling to room temperature, the mixture was extracted with DCM for 3 times. The organic layer was dried with anhydrous sodium sulfate, and the solvent was removed on a rotavapor. The crude product was separated by silica gel column chromatography with hexane / ethyl acetate (15:1, v/v) as the eluent. The orange solid was the final product (0.11 g, yield 15%). <sup>1</sup>H NMR (400 MHz, CDCl<sub>3</sub>) δ 8.49 (s, 2H), 8.33 (d, *J* = 8.0 Hz, 2H), 7.96 (d, *J* = 8.1 Hz, 2H), 7.48 (d, *J* = 8.4 Hz, 4H), 7.17 - 7.01 (m, 14H), 6.93 (dd, *J* = 15.4, 8.7 Hz, 8H), 6.62 (dd, *J* = 11.7, 8.7 Hz, 8H), 3.86 (d, *J* = 3.3 Hz, 8H), 3.44 (ddd, *J* = 49.8, 15.7, 6.8 Hz, 8H), 1.87 - 1.67 (m, 16H), 1.40 (s, 16H), 1.27 (d, *J* = 6.3 Hz,

32H). MALDI-TOF-MS (m/z): calcd for  $[\text{C}_{106}\text{H}_{121}\text{Br}_4\text{O}_6 + \text{H}]^+$ : 1810.5889, found: 1810.831.

#### 4.3.5 Synthesis of BTPEAQ-10.

Compound D (0.12 g, 0.07 mmol) was dissolved in pyridine (80 mL). The mixture was refluxed at 110 °C for 48 h. The solvent was removed on a rotavapor. Then the product was washed for 5 times with ethyl ether. The crimson solid was the final product (0.11 g, yield 76%).  $^1\text{H}$  NMR (600 MHz, DMSO- $d_6$ )  $\delta$  9.09 (dd,  $J = 12.3, 5.7$  Hz, 8H), 8.63 - 8.56 (m, 4H), 8.39 (s, 2H), 8.27 (d,  $J = 8.2$  Hz, 2H), 8.21 (d,  $J = 8.7$  Hz, 2H), 8.19 - 8.10 (m, 8H), 7.69 (d,  $J = 8.3$  Hz, 4H), 7.21 - 7.10 (m, 10H), 7.01 (d,  $J = 7.4$  Hz, 4H), 6.92 (d,  $J = 8.6$  Hz, 4H), 6.87 (d,  $J = 8.3$  Hz, 4H), 6.70 (dd,  $J = 23.9, 8.7$  Hz, 8H), 4.58 (dt,  $J = 15.0, 7.4$  Hz, 8H), 3.86 (t,  $J = 6.1$  Hz, 8H), 1.90 (dd,  $J = 18.3, 7.3$  Hz, 8H), 1.64 (d,  $J = 6.5$  Hz, 8H), 1.32 (d,  $J = 39.6$  Hz, 16H), 1.23 (s, 32H). ESI-MS (m/z): calcd for  $[\text{C}_{126}\text{H}_{140}\text{N}_4\text{O}_6]^{4+}$ : 451.5202, found: 451.5199.

#### 4.4 Cell viability assay

The viability of HeLa cells was evaluated by CCK-8 method, where BTPEAQ-10 and co-assemblies of BTPEAQ-10 and SDBS were separately co-cultured with the HeLa cells at 37 °C and with existence of 5%  $\text{CO}_2$ . Note that the HeLa cells were pre-cultured in the mediums without the fluorescent probes for 12 h. In the following, the pre-cultured cells were cultured in the mediums with the fluorescent probes for 12 h. Herein,  $C_B$  was varied as 0, 2, 4, 8, 12, 16,  $32 \times 10^{-6}$  mol  $\text{L}^{-1}$ , and  $C_S$  was 4-fold of  $C_B$ . Then 10  $\mu\text{L}$  of CCK-8 solution was added and continuously cultured for 2 h. The absorbance (i.e. OD value) at 450 nm was measured by using a microplate reader (Spectramax i3, Molecular Devices, USA). For each condition, three groups of cells were parallel tested. The biocompatibility was evaluated by comparing the viability of the cells treated with the fluorescent probes with the control.

#### 4.5 Cell culturing and imaging

HeLa cells were cultured in Dulbecco's Modified Eagle Medium (DMEM, ThermoFisher) and 10% fetal bovine serum for 12 h. The pre-cultured cells were then cultured in the mediums with BTPEAQ-10 ( $C_B = 5 \times 10^{-6} \text{ mol L}^{-1}$ ) or BTPEAQ-10 & SDBS ( $C_B = 5 \times 10^{-6} \text{ mol L}^{-1}$ ,  $C_S = 20 \times 10^{-6} \text{ mol L}^{-1}$ ) for 2 h, and then gently washed with phosphate buffered saline for 3 times and fixed with 2% paraformaldehyde for 40 min. The cells were imaged with CLSM. (Excitation wavelength: 405 nm).

#### Acknowledgements

We thank the financial support from the National Natural Science Foundation of China (21674075), the Natural Science Foundation of Jiangsu Province (BK20161211), and the Key University Science Research Project of Jiangsu Province (17KJA150007). This project is also supported by the Jiangsu Key Laboratory for Carbon-Based Functional Materials & Devices, at Soochow University.

#### References

- [1] Chen X-M, Chen Y, Yu Q, Gu B-H, Liu Y. Supramolecular Assemblies with Near-Infrared Emission Mediated in Two Stages by Cucurbituril and Amphiphilic Calixarene for Lysosome-Targeted Cell Imaging. *Angew Chem Int Ed.* 2018;57(38):12519-23.
- [2] Peng H-Q, Niu L-Y, Chen Y-Z, Wu L-Z, Tung C-H, Yang Q-Z. Biological Applications of Supramolecular Assemblies Designed for Excitation Energy Transfer. *Chem Rev.* 2015;115(15):7502-42.
- [3] Palivan CG, Goers R, Najer A, Zhang X, Car A, Meier W. Bioinspired polymer vesicles and membranes for biological and medical applications. *Chem Soc Rev.* 2016;45(2):377-411.

- [4] Li B, He T, Shen X, Tang D, Yin S. Fluorescent supramolecular polymers with aggregation induced emission properties. *Polym Chem.* 2019;10(7):796-818.
- [5] Saha PC, Chatterjee T, Pattanayak R, Das RS, Mukherjee A, Bhattacharyya M, et al. Targeting and Imaging of Mitochondria Using Near-Infrared Cyanine Dye and Its Application to Multicolor Imaging. *ACS Omega.* 2019;4(11):14579-88.
- [6] Hyun H, Park MH, Owens EA, Wada H, Henary M, Handgraaf HJM, et al. Structure-inherent targeting of near-infrared fluorophores for parathyroid and thyroid gland imaging. *Nat Med.* 2015;21(2):192-7.
- [7] Gao M, Wang R, Yu F, Li B, Chen L. Imaging of intracellular sulfane sulfur expression changes under hypoxic stress via a selenium-containing near-infrared fluorescent probe. *J Mater Chem B.* 2018;6(41):6637-45.
- [8] Wang T, Chai Y, Chen S, Yang G, Lu C, Nie J, et al. Near-infrared fluorescent probe for imaging nitroxyl in living cells and zebrafish model. *Dyes Pigments.* 2019;166:260-5.
- [9] Shi Y, Meng X, Yang H, Song L, Liu S, Xu A, et al. Lysosome-specific sensing and imaging of pH variations in vitro and in vivo utilizing a near-infrared boron complex. *J Mater Chem B.* 2019;7(22):3569-75.
- [10] Owens EA, Henary M, El Fakhri G, Choi HS. Tissue-Specific Near-Infrared Fluorescence Imaging. *Acc Chem Res.* 2016;49(9):1731-40.
- [11] Sreejith S, Joseph J, Lin M, Menon NV, Borah P, Ng HJ, et al. Near-Infrared Squaraine Dye Encapsulated Micelles for in Vivo Fluorescence and Photoacoustic Bimodal Imaging. *ACS Nano.* 2015;9(6):5695-704.
- [12] Pu K-Y, Li K, Liu B. A Molecular Brush Approach to Enhance Quantum Yield and

- Suppress Nonspecific Interactions of Conjugated Polyelectrolyte for Targeted Far-Red/Near-Infrared Fluorescence Cell Imaging. *Adv Funct Mater.* 2010;20(17):2770-7.
- [13] Frangioni J. In vivo near-infrared fluorescence imaging. *Curr Opin Chem Biol.* 2003;7(5):626-34.
- [14] König K. Multiphoton microscopy in life sciences. *J Microsc.* 2000;200:83-104.
- [15] Wang J, Hang Y, Hua J. Mannose-functionalized diketopyrrolopyrrole as AIE-active probes for lectin detection and cancer cell imaging. *Sens Actuators, B.* 2019;282:232-42.
- [16] Li X, Gao X, Shi W, Ma H. Design Strategies for Water-Soluble Small Molecular Chromogenic and Fluorogenic Probes. *Chem Rev.* 2014;114(1):590-659.
- [17] Zhang M, Zheng S-t, Liu X-j, Long Y, Yang B-q. A series of novel NIR fluorescent dyes: Synthesis, theoretical calculations and fluorescence imaging applications in living cells. *Dyes Pigments.* 2016;125:220-8.
- [18] Shi H, Liu J, Geng J, Tang BZ, Liu B. Specific Detection of Integrin  $\alpha_v\beta_3$  by Light-Up Bioprobe with Aggregation-Induced Emission Characteristics. *J Am Chem Soc.* 2012;134(23):9569-72.
- [19] Liu Y, Niu L-Y, Liu X-L, Chen P-Z, Yao Y-S, Chen Y-Z, et al. Synthesis of N,O,B-Chelated Dipyromethenes through an Unexpected Intramolecular Cyclisation: Enhanced Near-Infrared Emission in the Aggregate/Solid State. *Chemistry-a European Journal.* 2018;24(51):13549-55.
- [20] Xia Y, Dong L, Jin Y, Wang S, Yan L, Yin S, et al. Water-soluble nano-fluorogens fabricated by self-assembly of bolaamphiphiles bearing AIE moieties: towards application in cell imaging. *J Mater Chem B.* 2015;3(3):491-7.

- [21] Zhou Z, Zhang CC, Zheng Y, Wang Q. Luminescence modulation of two individual fluorophores over a wide pH range and intracellular studies. *Dyes Pigments*. 2018;150:151-7.
- [22] Zhao C-M, Wang K-R, Wang C, He X, Li X-L. Cooling-Induced NIR Emission Enhancement and Targeting Fluorescence Imaging of Biperylene Monoimide and Glycodendrimer Conjugates. *ACS Macro Lett*. 2019;8(4):381-6.
- [23] Ding L, Zhou S, Li D, Wu C, Xing Y, Song B. A facile method to incorporate tetraphenylethylene into polymeric amphiphiles: High emissive nanoparticles for cell-imaging. *Dyes Pigments*. 2019;160:711-6.
- [24] Ran X, Wang Z, Pu F, Liu Z, Ren J, Qu X. Aggregation-induced emission-active Au nanoclusters for ratiometric sensing and bioimaging of highly reactive oxygen species. *Chem Commun*. 2019;55(100):15097-100.
- [25] Weil T, Vosch T, Hofkens J, Peneva K, Muellen K. The Rylene Colorant Family-Tailored Nanoemitters for Photonics Research and Applications. *Angew Chem Int Ed*. 2010;49(48):9068-93.
- [26] Zhan X, Facchetti A, Barlow S, Marks TJ, Ratner MA, Wasielewski MR, et al. Rylene and Related Diimides for Organic Electronics. *Adv Mater*. 2011;23(2):268-84.
- [27] Shen XY, Yuan WZ, Liu Y, Zhao Q, Lu P, Ma Y, et al. Fumaronitrile-Based Fluorogen: Red to Near-Infrared Fluorescence, Aggregation-Induced Emission, Solvatochromism, and Twisted Intramolecular Charge Transfer. *J Phys Chem C*. 2012;116(19):10541-7.
- [28] Feng G, Wu W, Xu S, Liu B. Far Red/Near-Infrared AIE Dots for Image-Guided Photodynamic Cancer Cell Ablation. *ACS Appl Mater Inter*. 2016;8(33):21193-200.

- [29] Shao L, Sun J, Hua B, Huang F. An AIEE fluorescent supramolecular cross-linked polymer network based on pillar[5]arene host-guest recognition: construction and application in explosive detection. *Chem Commun.* 2018;54(38):4866-9.
- [30] Huang L, Dai L. Aggregation-Induced Emission for Highly Selective and Sensitive Fluorescent Biosensing and Cell Imaging. *J Polym Sci, Part A: Polym Chem.* 2017;55(4):653-9.
- [31] Hong Y, Lam JWY, Tang BZ. Aggregation-induced emission. *Chem Soc Rev.* 2011;40(11):5361-88.
- [32] Zhou J, Yu G, Huang F. AIE opens new applications in super-resolution imaging. *J Mater Chem B.* 2016;4(48):7761-5.
- [33] Long R, Tang C, Xu J, Li T, Tong C, Guo Y, et al. Novel natural myricetin with AIE and ESIPT characteristics for selective detection and imaging of superoxide anions in vitro and in vivo. *Chem Commun.* 2019;55(73):10912-5.
- [34] Gao M, Sim CK, Leung CWT, Hu Q, Feng G, Xu F, et al. A fluorescent light-up probe with AIE characteristics for specific mitochondrial imaging to identify differentiating brown adipose cells. *Chem Commun.* 2014;50(61):8312-5.
- [35] Zhang F, Di Y, Li Y, Qi Q, Qian J, Fu X, et al. Highly efficient Far Red/Near-Infrared fluorophores with aggregation-induced emission for bioimaging. *Dyes Pigments.* 2017;142:491-8.
- [36] Yu DF, Zhang Q, Wu CX, Wang YX, Peng LH, Zhang DQ, et al. Highly Fluorescent Aggregates Modulated by Surfactant Structure and Concentration. *J Phys Chem B.* 2010;114(27):8934-40.

- [37] Faul CFJ, Antonietti M. Ionic Self-assembly facile synthesis of supramolecular materials. *Adv Mater.* 2003;15:673-83.
- [38] Zhou S, Zhang L, Feng Y, Li H, Chen M, Pan W, et al. Fullerenols Revisited: Highly Monodispersed Photoluminescent Nanomaterials as Ideal Building Blocks for Supramolecular Chemistry. *Chem - Eur J.* 2018;24(62):16609-19.
- [39] Iwunze MO. Media influence on the enhancement of the fluorescence of berberine hydrochloride. *Monatsh Chem.* 2000;131:429-35.
- [40] Acharya S, Reberly B. Fluorescence spectrometric study of eosin yellow dye-surfactant interactions. *Arab J Chem.* 2009;2(1):7-12.
- [41] Du J, Zhao D, Chen Y-G, He Z-K. Effects of different surfactants on fluorescent properties and charge transfer of conjugated polymer. *Acta Chim Sinica.* 2006;64(10):963-7.
- [42] Mitani M, Yoshio M, Kato T. Tuning of luminescence color of  $\pi$ -conjugated liquid crystals through co-assembly with ionic liquids. *J Mater Chem C.* 2017;5(38):9972-8.
- [43] Evans RC, Knaapila M, Willis-Fox N, Kraft M, Terry A, Burrows HD, et al. Cationic Polythiophene-Surfactant Self-Assembly Complexes: Phase Transitions, Optical Response, and Sensing. *Langmuir.* 2012;28(33):12348-56.
- [44] Lorena Cortez M, Pallarola D, Ceolin M, Azzaroni O, Battaglini F. Ionic self-assembly of electroactive biorecognizable units: electrical contacting of redox glycoenzymes made easy. *Chem Commun.* 2012;48(88):10868-70.
- [45] Akram M, Anwar S, Kabir Ud D. Biophysical investigation of promethazine hydrochloride binding with micelles of biocompatible gemini surfactants: Combination of spectroscopic and electrochemical analysis. *Spectrochimica Acta Part A.* 2019;215:249-59.

- [46] Zheng D, Fan J, Huang X, Ding L, Xin Y. Fluorescent binary ensemble with pattern recognition ability for identifying multiple metalloproteins with applications in serum and urine. *RSC Adv.* 2017;7(79):50097-105.
- [47] Dutta R, Ghosh S, Banerjee P, Kundu S, Sarkar N. Micelle-vesicle-micelle transition in aqueous solution of anionic surfactant and cationic imidazolium surfactants: Alteration of the location of different fluorophores. *J Colloid Interface Sci.* 2017;490:762-73.
- [48] Ghosh R, Das S, Chatterjee DP, Nandi AK. Surfactant-Triggered Fluorescence Turn "on/off" Behavior of a Polythiophene-graft-Polyampholyte. *Langmuir.* 2016;32(33):8413-23.
- [49] Kumar S, Singh P, Mahajan A, Kumar S. Aggregation Induced Emission Enhancement in Ionic Self-Assembled Aggregates of Benzimidazolium Based Cyclophane and Sodium Dodecylbenzenesulfonate. *Org Lett.* 2013;15(13):3400-3.
- [50] Duan X-F, Zeng J, Lu J-W, Zhang Z-B. A facile synthesis of tetraarylethenes via cross McMurray coupling between diaryl ketones. *Synthesis.* 2007;5:713-8.
- [51] Zhao E, Chen Y, Wang H, Chen S, Lam JWY, Leung CWT, et al. Light-Enhanced Bacterial Killing and Wash-Free Imaging Based on AIE Fluorogen. *ACS Appl Mater Inter.* 2015;7(13):7180-8.
- [52] Kuwabara T, Orii J, Segawa Y, Itami K. Curved Oligophenylenes as Donors in Shape-Persistent Donor-Acceptor Macrocycles with Solvatochromic Properties. *Angew Chem Int Ed.* 2015;54(33):9646-9.

## Highlights

1. A four-armed amphiphile with near-infrared emission is synthesized.
2. The fluorescence emission is greatly enhanced by ionic co-assembly.
3. The co-assemblies are successfully applied in fluorescent labeling of HeLa cells.

Journal Pre-proof

**Declaration of interests**

The authors declare that they have no known competing financial interests or personal relationships that could have appeared to influence the work reported in this paper.

The authors declare the following financial interests/personal relationships which may be considered as potential competing interests:

Journal Pre-proof